New Journal of Physics
The open–access journal for physics

Photon emission spectroscopy of thin MgO films with the STM: from a tip-mediated to an intrinsic emission characteristic

H-M Benia, P Myrach and N Nilius[1]
Fritz-Haber-Institut der Max-Planck-Gesellschaft Faradayweg 4-6,
D-14195 Berlin, Germany
E-mail: nilius@fhi-berlin.mpg.de

New Journal of Physics **10** (2008) 013010 (9pp)
Received 4 September 2007
Published 17 January 2008
Online at http://www.njp.org/
doi:10.1088/1367-2630/10/1/013010

Abstract. Electron injection from the tip of a scanning tunnelling microscope (STM) has been used to stimulate local photon emission from the surface of a thin MgO film grown on Mo(001). Depending on the excitation energy, several emission regimes have been identified on the basis of the energy and the spatial distribution of the emitted photons. At low excitation bias, tip-induced plasmons are excited in the tip–sample gap, carrying little information on the oxide film. With increasing tip bias, radiative electron transitions between field-emission resonances dominate the photon response from the MgO surface. Intrinsic optical modes of the oxide material, such as radiative decays of electron–hole pairs, are only observed when operating the STM in the field emission regime, where the direct correlation between the photon signal and the local surface morphology gets partially lost due to the increased tip–sample distance.

Light emission spectroscopy with the scanning tunneling microscope (STM) has evolved into a powerful tool to measure optical properties of a sample surface with nanometre spatial resolution [1]. In contrast to classical absorption/emission spectroscopy, it allows direct correlation between the optical characteristic and the structural properties of the emitting entity. This is especially important for inhomogeneous samples, where the size and shape distribution of nano-objects and the presence of statistical disorder lead to inhomogeneous broadening effects in averaging optical techniques. Consequently, an STM-based approach has been chosen to explore the optical properties of individual species, selected from an ensemble of metal particles [2], semiconductor quantum dots [3] or molecules [4]–[6].

[1] Author to whom any correspondence should be addressed.

The application of local techniques is also desirable for the optical analysis of wide-gap insulators, such as alkali halogenides or alkali earth oxides. Their optical response is strongly related to the presence of imperfections in the crystal lattice, e.g. defects or low coordinated sites [7]–[9], and should exhibit pronounced spatial variations across the sample surface. Structural defects in wide-gap insulators act as trapping centres for electron–hole pairs (excitons), which then decay via the emission of photons with trap-specific energies [10]. Thus far, correlation between the various defect types on the surface (vacancies, corner or step sites) and their optical signature is only based on a combination of non-local optical spectroscopy and model calculations, and relies on the comparison of measured and calculated photon energies. To verify this assignment on a purely experimental base, local structural and optical information has to be acquired from the insulator surface, which is in principle feasible using light emission spectroscopy with the STM.

In a previous paper, we have demonstrated that electron injection from an STM tip can indeed be used to stimulate photon emission from an MgO surface [11]. The problem of negligible conductivity of wide-gap materials was circumvented in this case by growing MgO films on a Mo(001) support [12]. The additional use of elevated sample bias (5.0–8.0 V) ensured sufficient electron transport to explore oxide films of up to 20 ML thickness. The detected photon energies from the MgO were found to be considerably smaller than expected for an exciton-mediated process (1.6 eV instead of 3.0–5.0 eV). This shift of the emission peak was related to a decisive role of the STM tip in the emission process, either via tip-induced plasmons (TIPs) in the tip–sample cavity [1, 13] or radiative transitions between field-emission resonances (FERs) that form in the tip electric field [14, 15]. For the gold tip used in that experiment, discrimination between the two scenarios was impossible, as both processes produce photons of similar energy. To clarify the emission mechanism, the influence of the tip material on the optical characteristic has to be explored: while the energy of TIP modes depends sensitively on both the tip and sample material [13], FERs remain largely unaffected when changing the tip material, as long as its work function is not drastically altered.

In a new set of experiments, we now use silver tips to measure the optical response from the MgO surface. Silver as tip material supports TIP modes that are considerably higher in energy than those of gold. As a side effect, also the field-enhancement in the tip–sample cavity peaks at higher frequencies, which might facilitate the detection of optical modes with higher energy, e.g. MgO excitons [6, 16]. The experiments with Ag tips reveal a crossover in the dominant luminescence channel, changing from a tip-induced to an exciton-mediated mechanism in the oxide film with increasing excitation energy.

The measurements are preformed with a Beetle-type STM operated in ultra-high vacuum (2×10^{-1} mbar) and at liquid nitrogen temperature (100 K). The STM head is surrounded by a parabolic mirror that collects photons from the tunnel junction and guides them through a quartz view port towards a second mirror outside the vacuum chamber. From there, the light is either reflected to a CCD-detector coupled to a grating spectrograph or to a photo-multiplier tube for wavelength-integrated measurements. The photo-multiplier is used to record photon-maps of the oxide surface. For this purpose, the sample is scanned with reduced speed ($\sim$20 nm s^{-1}) and enabled feedback loop and the photo-multiplier signal is detected at each pixel of the image. To increase the signal-to-noise ratio, the photon signal is low-pass filtered before being read into the STM controller. As topographic and photon maps are measured simultaneously, the spatial arrangement of emission centres on the surface becomes accessible to the experiment and can be assigned to structural features.

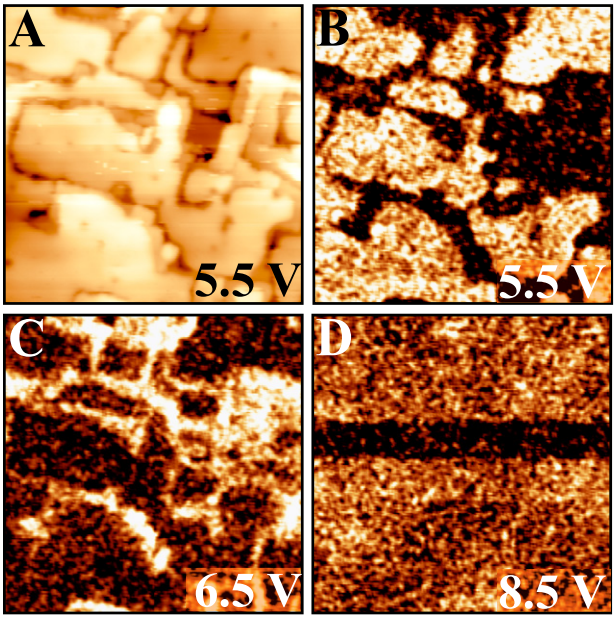

Figure 1. (A) Topographic image and (B)–(D) corresponding photon maps of a 7 ML thick MgO film on Mo(001) (size $50 \times 50\,\mathrm{nm}^2$). A constant current of 2.0 nA was used in all measurements. For some lines in the upper half of image (D), a smaller current of 0.2 nA was used to define the dark level of the photon signal.

The MgO films are prepared by Mg deposition onto a sputtered/flashed Mo(001) surface in 1×10^{-7} mbar O_2 at room temperature. The film is then annealed to 820 K in vacuum to ensure a crystalline and defect poor structure. The film thickness is deduced from STM images taken at sub-monolayer coverage and LEED measurements, displaying spot patterns that are characteristic for a distinct number of layers [12]. Direct height measurements with the STM are difficult for thick films, because the STM has to be operated in the near-field emission regime ($eU_{\mathrm{sample}} >$ work function) due to the insulating nature of MgO. At this condition, FERs in the tip–sample gap carry a large portion of the tunnel current and the measured height depends on their availability for electron transport [14]. Consequently, the tip height above the surface is not a good measure for the actual topographic height any more. We will therefore refer to the nominal MgO thickness, which has been adjusted to 7 ML in all experiments.

Figure 1(A) shows an STM topographic image of the MgO film taken at 5.5 V sample bias. The surface morphology is dominated by large rectangular oxide terraces of 20–50 nm size, separated by grooves that run along the [001] direction. In images taken at lower bias, these grooves are identified as screw dislocations, which are inserted into the film to release stress and strain related to the 5% lattice mismatch with the Mo support [12]. Photon maps, measured at the same position as the topographic image in figure 1(A), are shown in figures 1(B)–(D) for three different voltages. At +5.5 V sample bias, high emission yield is observed for tip positions above extended MgO islands. With increasing bias, the contrast reverses and oxide patches in the vicinity of dislocation lines start to emit light. Above +7.0 V sample bias, the contrast in the photon maps gradually vanishes and the emission becomes homogeneously distributed across the surface. However, even at elevated bias the MgO emits photons, as manifested by the

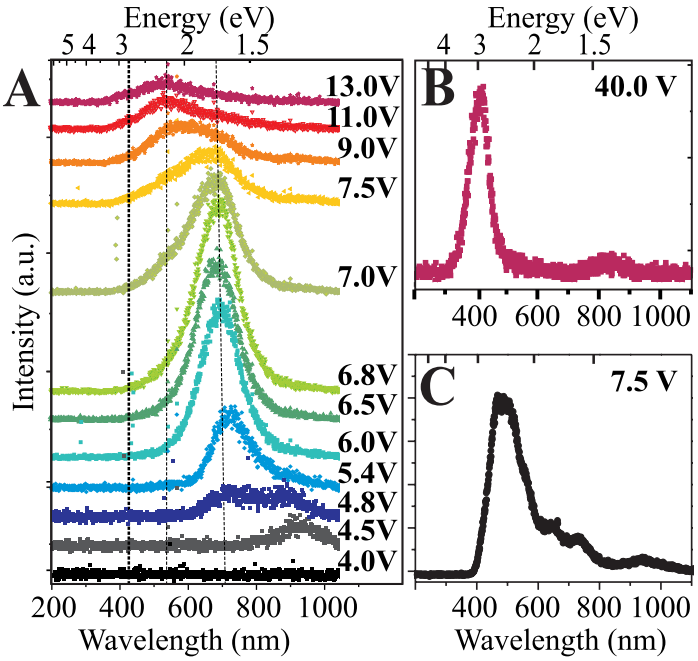

Figure 2. (A) Electro-luminescence spectra from a large MgO island on Mo(001) taken as a function of excitation bias. The electron current was set to 2 nA, the accumulation time per spectrum to 120 s. (B) Emission spectrum taken in the field emission regime ($U_{tip} = -40$ V, 1 nA, 60 s). (C) Photon spectrum with a large contribution of higher FERs in the emission process (2 nA, 120 s, details see text).

dark lines in figure 1(D) that are caused by a temporal decrease of the electron current. Photon mapping of the MgO is possible in the bias range from 4.5 to 14.0 V. For even higher excitation voltages, the tip can only be positioned at selected points above the surface, whereas scanning becomes unstable.

To identify the nature of the light emission from MgO thin films, the wavelength distribution of the emitted photons is analysed with the help of the CCD detector. Figure 2 presents a spectral series taken from a large MgO island as a function of sample bias. A strong dependence on the excitation bias is observed for both, the maximum position and the intensity of the emitted radiation. At the emission onset at around 4.5 V, a single peak appears in the spectrum at 920 nm (1.35 eV) that gradually shifts to lower wavelengths with increasing voltage. This trend is interrupted around 5.0 V, when a second peak emerges at 700 nm (1.8 eV) in the spectra and quickly develops into the dominant feature. The peak intensity runs through a pronounced maximum at 6.5–6.8 V excitation bias without changing its wavelength position and declines again with further bias increase. At 7.0 V, the 700 nm peak has weakened so much that a faint shoulder becomes visible at 500 nm (2.5 eV), which develops into a broad peak that is detectable over a large bias range. Additional photon intensity between 400 and 500 nm is observed for excitation voltages above 10 V, however, no sharp spectral feature can be distinguished and the total emission cross-section remains small. Only in the far field-emission regime ($-25\,\text{V} < V_{tip} < -100\,\text{V}$), another emission peak emerges at 400 nm (3.1 eV) in the spectra (figure 2(B)). Its intensity increases exponentially with excitation bias. To visualize

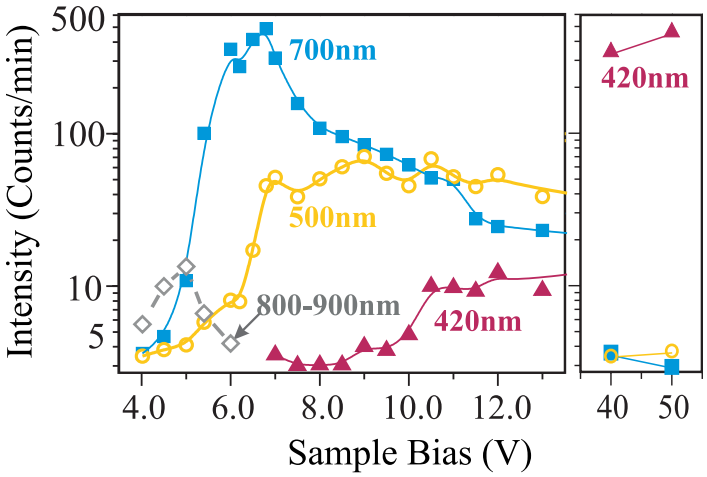

Figure 3. Evolution of the emission cross-section with excitation bias for selected wavelengths. The plot is derived from deconvoluting the spectral series shown in figure 2 into a set of Gaussian peaks. A logarithmic scale is used for the intensity axis.

the evolution of the different spectral components as a function of bias, the emission spectra are deconvoluted into a set of Gaussian-shaped peaks. A combination of three Gaussians is sufficient to obtain a satisfying reproduction of the intensity distribution for all voltages. The evolution of the main peaks with sample bias, as derived from the fitting procedure, is summarized in figure 3.

The complex spectral behaviour of the STM junction consisting of an MgO/Mo sample and an Ag tip does not follow a single emission mechanism, but involves several channels that are active in different energy windows. The long-wavelength emission detected for low excitation bias is neither compatible with the intrinsic MgO emission nor with optical modes excited in the silver tip. Based on its distinct blue-shift and intensity decrease with increasing sample bias, the emission is assigned to coupled plasmon modes excited in the STM cavity, so called TIPs [1]. Such TIP modes can be viewed as coherent oscillations of the conduction electrons in tip and sample, which are driven by inelastic tunnelling processes and efficiently couple to photons. Their resonance behaviour is determined by the dielectric properties of tip and sample material and can be approximated by solving the Laplace equation for the electromagnetic potentials between a metal sphere (tip) and a metal surface [13]. In the present case, only the Ag tip and the Mo sample are actively involved in TIP excitations, because the oxide film has a negligible free-electron density. A distinct influence of the dielectric MgO layer on the emission characteristic is, however, concluded from two experimental observations. First, the onset bias of 4.5 V is unusually high for TIP-mediated emission, which starts at much lower voltages in pure metal–metal junctions [13, 17]. Taking only energy conservation arguments into account, the onset is expected to be at 1.3 V, when electrons have formally enough energy to excite the 900 nm photons. The high onset bias in the present case is attributed to the absence of final states for inelastically tunnelling electrons inside the MgO bandgap. The excitation probability for TIP modes is small, as long as tunnelling electrons have not enough energy to reach the MgO conduction band after an energy transfer to the TIP. From this consideration, the position of the conduction bandedge can be determined from the difference between onset bias and TIP energy

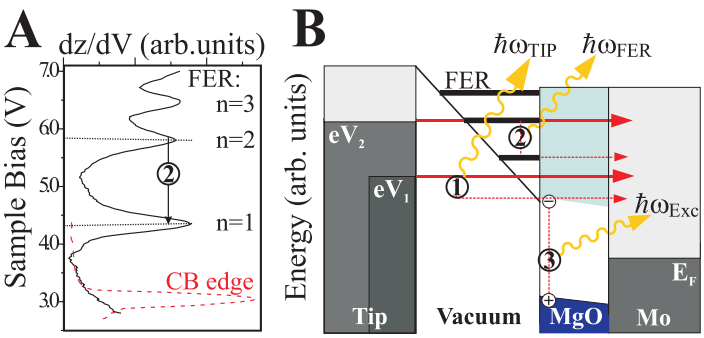

Figure 4. (A) $\mathrm{d}z/\mathrm{d}V$ spectra taken on top of a large MgO island on Mo(001) ($I = 50$ pA). While the maximum in the dashed curve marks the onset of the MgO conduction band, the solid line covers the range of the lower FERs. (B) Sketch of emission processes that might contribute to the photon signal from an Ag-tip/MgO/Mo(001) junction. The change in tip–sample distance with bias voltage is omitted for clarity. Channel 1 corresponds to a TIP-mediated process (bias V_1), channel 2 marks the transition between two FERs at bias V_2 and channel 3 illustrates the radiative decay of an electron–hole pair. Solid and dashed horizontal lines denote elastically and inelastically tunnelling electrons, respectively.

to be at 3.2 eV (4.5–1.3 eV). This value is verified by elastic tunnelling spectroscopy, where a pronounced peak at 3.1 eV marks the onset for electron transport into the MgO conduction band (figure 4(A), dashed line). Assuming E_F to be in the midgap position, a total bandgap of 6.4 eV is deduced for the 7 ML MgO film, which is smaller than the bulk value of 7.8 eV [18].

A second effect of the MgO is concluded from the energy of TIP modes. Whereas at the emission onset, the spectral position is given by the maximum energy transfer from tunnelling electrons (1.3 eV in the present case), it depends primarily on the dielectric properties of the tip/sample material beyond this energy constraint. For an Ag–Mo junction without MgO film, the TIP position is computed to 350 nm (3.5 eV), using the model described in [13]. No emission line is detected in this wavelength region. The only spectral feature compatible with a fully developed TIP mode would be the broad 500 nm (2.5 eV) peak, implying a red-shift of 1 eV compared to the theoretical value. Such deviation is, however, expected from the influence of the MgO film on the plasmon position. The dielectric layer increases the polarizability of the tip–sample cavity with respect to a vacuum gap ($\varepsilon_{\mathrm{MgO}} = 10$ versus $\varepsilon_{\mathrm{Vac}} = 1$) and shifts the TIP mode to lower energies. A similar behaviour is well known for plasmon polaritons in metal particles that are embedded in a matrix with a high dielectric constant [19]. The assignment of the 500 nm peak to TIPs in the tunnel junction is, however, not beyond doubt, as the tip–sample separation at the excitation bias is already large and the electromagnetic coupling between both electrodes is correspondingly small. As discussed below, also an alternative emission process might account for this spectral feature.

The emission peak at 700 nm is not compatible with a TIP-mediated process, because neither its sharp intensity variation with sample bias, nor its constant peak position fit into the general picture of coupled plasmon modes. Its appearance falls into the energy window, where FERs start to control the electron transport between tip and sample. FERs occur at bias voltages exceeding the sample work function, when electrons from the tip leave the tunnel barrier and

propagate as free carriers on their trajectory to the sample [14, 20]. Whenever multiples of half the free-electron wavelength match the distance between tunnel barrier and MgO surface, the electrons form standing waves in the gap, the FERs (figure 4(B)). Electron transport through such resonances is extremely efficient and causes a step-like increase in the conductance at each FER level. The associated retraction of the tip from the surface when running through a FER with closed feedback loop can be used to determine its bias position in tip-height versus voltage (dz/dV) spectra (figure 4(A)). The MgO film gives rise to FERs with long electron lifetimes due to the small penetration probability of electrons into the insulating oxide and the limited number of alternative propagation channels. As a result, radiative transitions of electrons between FER levels become possible and contribute to the photon response from the MgO surface[2]. This mechanism is comparable to the light emission observed from quantum well states in a Na overlayer on Cu(111) [21], but rather untypical for normal metal junctions due to the presence of efficient non-radiative recombination channels.

An involvement of FERs in the MgO emission characteristic produces a distinct spectral signature that can be verified experimentally. (i) The emission should start at bias voltages where the 2nd FER is populated and electrons can radiatively decay into the 1st level. (ii) The observed photon energy should be nearly independent of the excitation bias, but fixed by the separation of the participating FER levels. (iii) The tip material only marginally affects the emission behaviour, in sharp contrast to a TIP-mediated process [13]. All these attributes of FER-mediated light are found in the characteristic of the 700 nm photon peak. (i) In dz/dV spectra taken on large MgO islands, the progression of FERs is clearly seen and their energy position can be deduced (figure 4(A)). Population of the 2nd FER and transition to the 1st level becomes possible at 5.5–6.0 V, in good agreement with the visibility onset of the 700 nm peak. (ii) The energy separation between the 2nd and 1st FER amounts to approximately 1.6 eV, which closely matches the energy of the photon peak (1.7 eV)[3]. (iii) A pronounced emission peak of comparable wavelength (∼750 nm) was also detected for the MgO/Mo system probed with an Au tip [11]. This similarity in the emission characteristic for both tip materials is not compatible with a TIP-mediated process, but supports an interpretation of the emission as being induced by radiative transitions between FERs. It should be emphasized that the bias range for exciting the 700 nm emission peak is not only determined by the intrinsic width of the FERs, but also related to variations in their energy position at different surface locations. FER levels occur at lower energy on spatially extended MgO patches, which therefore start to emit light at relatively small bias voltage (photon map in figure 1(B)). Low-lying FERs are compatible with a small work function of the defect-free MgO islands, which relates to the oxide-induced quenching of the Mo surface dipole as one origin of the sample work function [22]. Around screw dislocations, this work function decrease is apparently less efficient, possibly because of non-compensated charges around the defect lines or a residual influence of the Mo support. As a result, FERs around dislocation lines shift to higher energies and those regions show up in the photon maps at larger sample bias (figure 1(C)).

[2] In a strictly one-dimensional (1D) picture, radiative transitions between FERs are dipole forbidden. The dipole selection rules are however softened by the influence of the tip and the resulting 3D character of FERs.

[3] The exact position of FERs depends on tip shape and tunnelling current and can vary by several tens of a volt in different experimental runs. Furthermore, the photon energy from transitions between FERs does not exactly correspond to the level separation deduced from dz/dV spectroscopy, as the tip–sample distance and therefore the FER energy changes during spectroscopy.

The 700 nm peak decreases sharply in intensity at bias voltages above 7.0 V, when electrons from the tip cannot populate the 2nd FER any more. However, higher levels become accessible for electron transport in this bias range and might contribute to the optical response. Electrons in the 3rd FER can undergo radiative transitions to the 1st and 2nd state, giving rise to photons of roughly 500 and 1500 nm wavelength, as deduced from the dz/dV spectra. Whereas the latter ones are outside the spectral window covered by the CCD detector, transitions between the 3rd and 1st FER should be observable in the experiment. Indeed, a step-like increase of the emission yield of 500 nm photons is observed at an excitation bias of 7.0 V, and, at least partly, assigned to the onset of radiative transitions involving higher FERs. A distinct spectral signature, as revealed for the 2nd to 1st FER transition, is not observed in this case. The absence of a sharp peak might be owed to the presence of competing decay channels for electrons in the 3rd FER, for instance easier penetration into the MgO film, transitions to the 2nd level, coupling to TIP modes of similar energy or enhanced scattering with electron–hole pairs in the Mo support. Only occasionally, transitions between the 3rd and 1st FER give rise to a pronounced emission peak as shown in figure 2(C). The morphological peculiarity of the MgO region that favours this particular recombination channel is not known.

At excitation voltages beyond 10 V, a third emission regime becomes distinguishable, characterized by a gradual shift of the spectral weight into the ultraviolet and the emergence of a new peak at 400 nm (figure 2(B)). The latter develops into the dominant feature in electro-luminescence spectra excited with electron energies above 30 eV, where any direct tip influence on the emission process is excluded due to the macroscopic tip–sample separation. Also the peak position points to an intrinsic property of the oxide film, as similar optical bands have been observed in earlier photo-luminescence measurements on MgO nano-crystals and smokes [7]–[9]. Based on DFT calculations [10], the emission was assigned to the radiative decay of excitons trapped at 3-fold coordinated oxygen ions located at corners and kinks of the MgO surface. Similar low-coordinated sites should be present in the MgO films on Mo(001), making an exciton-mediated emission channel also relevant for the interpretation of the present data. Excitons are stimulated by impact ionization of valence-band states via the injected electrons, which requires minimum excitation energy of the size of the MgO bandgap. However, measurable excitation cross-sections are only achieved at considerably higher impact energies [23], which suggests the importance of secondary processes, such as electron cascades and Auger decays for the exciton stimulation. The visibility of the 400 nm photon peak only for excitation energies above 10 eV is therefore not in conflict with exciton-mediated light emission. Further support for the peak assignment was earlier provided by the fact that small amounts of Au efficiently quench the emission, because Au particles block the trap sites for excitons in the MgO surface [24].

In conclusion, different light emission mechanisms have been identified in an STM junction containing an MgO thin film. At low sample bias, the optical response is determined by TIPs that form between the Ag tip and Mo support. The dominant emission channel changes at bias voltages at which electron transport in the junction is determined by FERs. Due to the insulating character of MgO, the FERs are sufficiently decoupled from the metal support to enable radiative electron transitions between higher and lower levels associated with the emission of photons. Intrinsic optical modes of the MgO, in particular excitons trapped at 3-fold coordinated anion sites, are stimulated only at high electron energies, where the tip–sample distance is large and the spatial resolution in the photon maps is not better than 1 nm. However, employing a combination of low-bias imaging and high-bias photon mapping might open a way

to gain indirect information on the atomic nature of the intrinsic emission centres in the MgO surface.

References

[1] Berndt R 1998 *Scanning Probe Microscopy (Springer Series in Nanoscience and Technology)* ed R Wiesendanger (Berlin: Springer) p 97
[2] Nilius N, Ernst N and Freund H-J 2000 *Phys. Rev. Lett.* **84** 3994
[3] Hakanson U, Johansson M K, Holm M, Pryor C, Samuelson L and Seifert W 2002 *Appl. Phys. Lett.* **81** 4443
[4] Qui X H, Nazin G V and Ho W 2003 *Science* **299** 542
[5] Cavar E, Blüm M-C, Pivetta M, Patthey F, Chergui M and Schneider W D 2005 *Phys. Rev. Lett.* **95** 196102
[6] Pettinger B 2006 *Top. Appl. Phys.* **103** 217
[7] Anpo M, Yamada Y, Kubokawa Y, Coluccia S, Zecchina A and Che M 1988 *J. Chem. Soc. Faraday Trans.* **84** 751
[8] Stankic S, Muller M, Diwald O, Sterrer M, Knözinger E and Bernardi J 2005 *Angew. Chem. Int. Edn. Engl.* **44** 4917
Stankic S, Bernardi J, Diwald O and Knözinger E 2006 *J. Phys. Chem.* B **110** 13866
[9] Hacquart R, Krafft J M, Costentin G and Jupille J 2005 *Surf. Sci.* **595** 172
[10] Shluger A L, Sushko P V and Kantorovich L N 1999 *Phys. Rev.* B **59** 2417
Sushko P V, Gavartin J L and Shluger A L 2002 *J. Phys. Chem.* B **106** 2269
[11] Benia H M, Nilius N and Freund H-J 2007 *Surf. Sci. Lett.* **601** L55
[12] Benedetti S, Benia H M, Nilius N, Valeri S and Freund H-J 2006 *Chem. Phys. Lett.* **430** 330
[13] Berndt R, Gimzewski J K and Johansson P 1993 *Phys. Rev. Lett.* **71** 3493
Johansson P, Monreal R and Apell P 1990 *Phys. Rev.* B **42** 9210
[14] Binnig G, Frank K H, Fuchs H, Garcia N, Reihl B, Rohrer H, Salvan F and Williams A R 1985 *Phys. Rev. Lett.* **55** 991
[15] Berndt R and Gimzewski J K 1993 *Ann. Phys.* **2** 133
[16] Wu S and Mills D L 2002 *Phys. Rev.* B **65** 205420
[17] Ito K, Ohyama S, Uehara Y and Ushioda S 1995 *Surf. Sci.* **324** 282
[18] Schintke S, Messerli S, Pivetta M, Patthey F, Libjoulle L, Stengel M, de Vita A and Schneider W D 2001 *Phys. Rev. Lett.* **87** 276801
[19] Kreibig U and Vollmer W 1995 *Optical Properties of Metal Clusters (Springer Series in Materials Science)* vol 25 (Berlin: Springer)
[20] Pitarke J M, Flores F and Echenique P M 1990 *Surf. Sci.* **234** 1
[21] Hoffmann G, Kliewer J and Berndt R 2001 *Phys. Rev. Lett.* **87** 176803
[22] Giordano L, Cinquini F and Pacchioni G 2005 *Phys. Rev.* B **73** 045414
[23] Berndt R and Gimzewski J 1992 *Phys. Rev.* B **45** 14095
[24] Benia H M, Lin X, Gao H J, Nilius N and Freund H-J 2007 *J. Phys. Chem.* C **111** 10528